ChemComm

COMMUNICATION

View Article Online
View Journal | View Issue

Cite this: *Chem. Commun.*, 2021, **57**, 2257

Received 23rd December 2020,
Accepted 25th January 2021

DOI: 10.1039/d0cc08328c

rsc.li/chemcomm

From a P_4 butterfly scaffold to *cyclo*- and *catena*-P_4 units†

Julian Müller, Gábor Balázs and Manfred Scheer *

The reactivity of $[\{Cp'''Fe(CO)_2\}_2(\mu,\eta^{1:1}\text{-}P_4)]$ (1) towards half-sandwich complexes of Ru(II), Rh(III), and Ir(III) is studied. The coordination of these Lewis acids leads to a rearrangement of the P_4 butterfly unit to form complexes with either an aromatic *cyclo*-P_4R_2 unit (R = $Cp'''Fe(CO)_2$) or a *catena*-tetraphosphaene entity.

The activation of small molecules is an active research topic. This research area focuses mainly on inert molecules such as H_2,[1,2] N_2,[1,3] CO_2,[4] and CH_4[1] since their functionalisation might be important to solve *e.g.* energy problems. However, this research area also includes highly reactive compounds such as white phosphorus (P_4) where the focus is to control its reactivity. In industrial applications, P_4 is an important starting material for the synthesis of organophosphorus derivatives. However, their synthesis proceeds *via* multistep reactions with low atom economic efficiency. To increase the sustainability, a direct and selective functionalization is desired. Therefore, the degradation of tetrahedral P_4 in the presence of reactive main group compounds[5] and transition metal complexes[6] is investigated (Scheme 1, top). Typically, harsh reaction conditions are needed to generate these reactive metal species.[7–12] In the field of P_4 conversion, work was done by the Scherer group, *e.g.* by showing that the photolysis of $[Cp''Fe(CO)_2]_2$ ($Cp'' = \eta^5\text{-}C_5H_3{}^tBu_2$) in the presence of P_4 leads to $[Cp''_2Fe_2(CO)_nP_4]$ (n = 3, 4 type **A**, n = 2 type **B**, n = 1 and n = 0 type **D**) by successive decarbonylation (Scheme 1, top).[8] Comparable results were obtained *via* thermolytic reactions of P_4 with $[Cp'''Fe(CO)_2]_2$[9] ($Cp''' = \eta^5\text{-}C_5H_2{}^tBu_3$), $[Cp^*Co(CO)_2]$[13] ($Cp^* = \eta^5\text{-}C_5Me_5$) and $[Cp^*Co(^iPr_2Im)(\eta^2\text{-}C_2H_4)]$[10,14] ($^iPr_2Im$ = 1,3-di-isopropylimidazolein-2-ylidene), respectively. The thermolysis of $[Cp^*Ni(CO)]_2$ leads to complexes of the type **E**.[15] In molten $GaCl_3$, P_4 can also be converted by *in situ* generated Ph_2P^+,[12] leading to the insertion of phosphonium cations into several P–P bonds to form cationic $P_4(PPh_2)$ (type **A**), $P_4(PPh_2)_2$ (type **C**) and $P_4(PPh_2)_3$ (type **F**) compounds.

Conversions of P_4 at mild conditions is an overall goal in this chemistry, which can be achieved with coordinative unsaturated complexes,[16,17] like the triple-decker complex $[(Cp'''Co)_2(\mu\text{-}C_7H_8)]$.[18] In solution it dissociates into the 14-valence-electron (VE) fragment $[Cp'''Co]$ and reacts readily with complexes bearing intact tetrahedral P_4 units to *cyclo*-P_4 (type **B**) containing derivatives.[16] On the other hand we showed that the formation of the butterfly complex $[\{Cp'''Fe(CO)_2\}_2(\mu,\eta^{1:1}\text{-}P_4)]$[9] (**1**) by the reaction of $[Cp'''Fe(CO)_2]_2$ with P_4 does not need thermal activation and already occurs quantitatively at room temperature.[19] The reactivity of **1** is very versatile, since the reaction with PhC≡CPh or P≡C^{t}Bu gives access to triphospholyl- and tetraphospholyl-containing iron complexes.[20] We could also show that **1** has the properties of a chelate ligand (Scheme 1, bottom, coordination type **I**).[21,22] Here, the P_4 butterfly scaffold coordinates to various transition metal-based

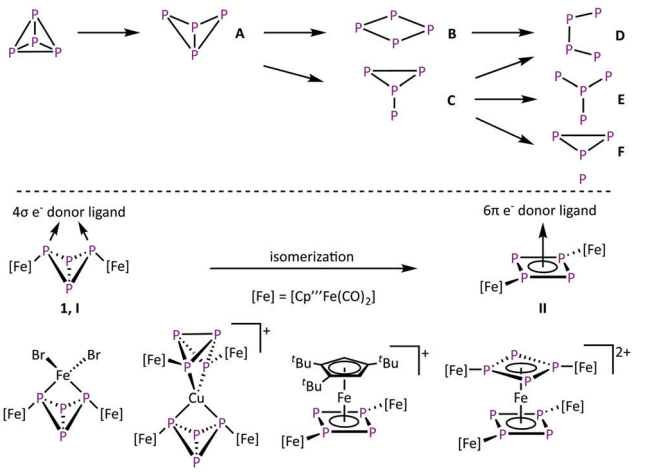

Scheme 1 Top: Schematic overview of the first steps of the successive degradation of the P_4 tetrahedron. Charges and lone pairs of electrons are omitted for the sake of simplicity. Bottom: Donor capabilities of **1** and selected examples of the resulting complexes.

Institut für Anorganische Chemie, Universität Regensburg, Regensburg 93040, Germany. E-mail: manfred.scheer@ur.de;
Web: http://www.uni-regensburg.de/chemie-pharmazie/anorganische-chemie-scheer/

† Electronic supplementary information (ESI) available. CCDC 2051733–2051736. For ESI and crystallographic data in CIF or other electronic format see DOI: 10.1039/d0cc08328c

Lewis acids *via* the two "wing tip" phosphorus atoms. However, in the presence of a d^6 metal Lewis acid like Fe(II) that bears ligands that can easily be substituted, an unusual isomerisation of the butterfly unit (4σ e^- donor, coordination type **I**) to an aromatic *cyclo*-P_4R_2 unit (6π e^- donor, R = [Cp′′′Fe(CO)$_2$], coordination type **II**) is observed, giving access to the unique homoleptic octaphosphorus sandwich complex $[\{(Cp'''Fe(CO)_2)_2(\mu_3,\eta^{4:1:1}\text{-}P_4)\}_2Fe][PF_6]_2$.[22a] To obtain deeper insight into the isomerisation reaction of **1**, it was reacted with various 3d metal Lewis acids to give mainly coordination as a chelating ligand, but in one case an isomerisation *via* a redoxreaction to Co(III) occurred.[22b] Since the availability of $3d^6$ metal-based Lewis acids like Fe(II) and Co(III) is limited, the question to use 4d and 5d transition metal complexes, which typically yield products with a higher stability, came into mind. This might alter the reaction outcome in general. Herein, we report on the reactivity of **1** towards Ru(II)-, Rh(III)-, and Ir(III)-based Lewis acids, surprisingly leading exclusively to an isomerisation to form *cyclo*- and also *catena*-P_4 containing complexes.

A method to generate unsaturated transition metal fragments in solution is to treat the corresponding metal halide precursor with an excess of a thallium(I) salt that bears a weakly coordinating anion to eliminate poorly soluble thallium(I) halides. This was used to generate the solvent-stabilized (CH_3CN or CH_2Cl_2) species "[CymRu][PF$_6$]$_2$" (Cym = *para*-cymene) and "[Cp*M][PF$_6$]$_2$" (M = Rh, Ir) *in situ*. These metal fragments react smoothly with **1** leading to $[\{Cp'''Fe(CO)_2\}_2(\mu_3,\eta^{4:1:1}\text{-}P_4)(LM)][PF_6]_2$ (**2**: LM = CymRu; **3**: LM = Cp*Rh; **4**: LM = Cp*Ir; Scheme 2). Complexes **2–4** feature all *cyclo*-P_4R_2 units that coordinate the central $[LM]^{2+}$ fragments. This finding reveals that the isomerisation of the P_4 butterfly moiety (4σ e^- donor, coordination type **I**) to a *cyclo*-P_4R_2 ligand (6π e^- donor, coordination type **II**) is a general feature, not only bound to 3d metals, if the 18 VE rule can be fulfilled and a d^6 metal is present. The molecular structures of **2–4** shows, that the central metal atom is coordinated in an η^4 fashion by the *cyclo*-P_4R_2 unit (Fig. 1). The similar covalent radii of Ru (r_{Ru} = 1.25 Å), Rh (r_{Rh} = 1.25 Å), and Ir (r_{Ir} = 1.22 Å) lead to similar M–$P_{4,cent.}$ distances of 1.8890(2) Å in **2**, 1.8939(3) Å in **3** and 1.8915(2) Å in **4**.[23] Compared to $[\{Cp'''Fe(CO)_2\}_2(\mu_3,\eta^{4:1:1}\text{-}P_4)(Cp'''Fe)][PF_6]$, the distances are approx. 0.13 Å longer (1.7609(5) Å) which is attributed

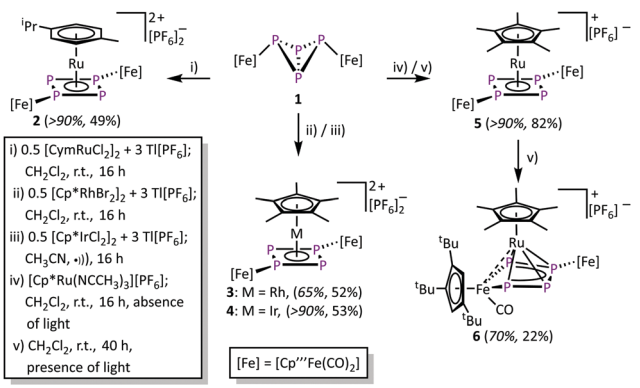

Scheme 2 Synthesis of the isomerisation products starting from **1**. The yields in italics are based on the ^{31}P NMR spectra of the crude reaction mixture, while the second value refers to the isolated yield.

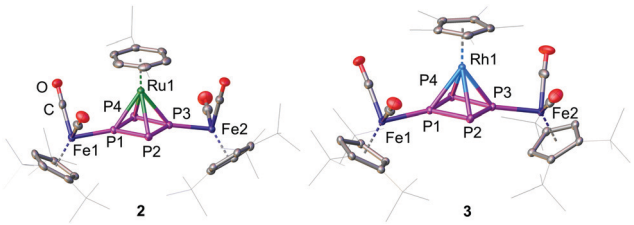

Fig. 1 Cationic parts of the molecular structures in solid state of **2** and **3**. The structural core of **3** exemplifies the one of **4** as well. Hydrogen atoms are omitted for clarity. A.d.p. are shown at 50% probability level.

to the smaller covalent radius of Fe (r_{Fe} = 1.16 Å).[22a] The P–P bond lengths are with 2.1356(7)–2.1481(7) Å (**2**), 2.1433(8)–2.1459(8) Å (**3**), and 2.1488(6)–2.1518(6) Å (**4**) in the range between a P–P single (2.20–2.25 Å) and a P=P double bond (2.00–2.05 Å). These bond lengths are in good agreement with the determined P–P distances in the isolated *cyclo*-P_4^{2-} anion (2.146(1) and 2.1484(9) Å) in $Cs_2P_4{\cdot}2NH_3$[24] as well as in other complexes with formal P_4^{2-} ligands.[16,22,25] The *cyclo*-P_4 units exhibit similar diamond-shaped geometries in all three complexes, which was also found in the other complexes derived from **1**.[22]

The ^{1}H NMR spectrum of **2** in CD_2Cl_2 shows two singlets at δ = 1.33 and 1.45 ppm and a multiplet at δ = 5.66 ppm with an integral ratio of 18 : 36 : 4 for the two Cp′′′ ligands. The signals at δ = 1.35, 2.59, and 6.71 ppm can be assigned to the Cym ligand. The ^{1}H NMR spectra of **3** and **4** show similar signals for the Cp′′′ ligands while the singlet of the Cp* signal can be detected at δ = 2.46 (**3**, CD_2Cl_2) and 2.64 ppm (**4**, CD_3CN), respectively. The $^{31}P\{^1H\}$ NMR spectra of **2** and **4** show each an AA′XX′ spin system for the cation (**2** in CD_2Cl_2: δ = 148.9 and 102.9 ppm; **4** in CD_3CN: δ = 102.3 and 62.7 ppm).‡ The cation of **3** shows two signals at δ = 169.8 and 121.1 ppm that are part of an AA′MM′X spin system (X corresponds to Rh) caused by the NMR-active ^{103}Rh nuclei (I = 1/2, 100% natural abundance).‡ However, the $^{31}P\{^1H\}$ NMR spectrum of the reaction solution of **3** reveals an additional set of signals at δ = 201.7, 157.7 and 125.7 ppm corresponding to a byproduct (AA′MNX spin system, X corresponds to Rh),‡ in a ratio of **3** to the byproduct of approximately 2 : 1. Despite several attempts, the exact structure of the byproduct could not be clarified yet, but, according to the NMR features, the presence of a *cyclo*-P_4 unit bound to a ^{103}Rh core is very likely.

The reaction of **1** and $[Cp^*Ru(NCCH_3)_3][PF_6]$ in the absence of light yields $[\{Cp'''Fe(CO)_2\}_2(\mu_3,\eta^{4:1:1}\text{-}P_4)(Cp^*Ru)][PF_6]$ (**5**). During this reaction, all acetonitrile ligands are substituted by **1**, while the P_4 core isomerises to a cyclic P_4 unit. Despite numerous attempts, it was not possible to isolate **5** in crystalline form. However, the $^{31}P\{^1H\}$ NMR spectrum of **5** in CD_2Cl_2 shows an AA′XX′ spin system at δ = 82.0 and 51.6 ppm unambiguously confirms its identity.‡ The chemical shift values as well as the spin system compare well to that found for **2–4** and $[\{Cp'''Fe(CO)_2\}_2(\mu_3,\eta^{4:1:1}\text{-}P_4)(Cp'''Fe)][PF_6]$[22] ($\delta$ = 78.9, 56.8 and 45.6 ppm).

Performing the reaction of **1** with $[Cp^*Ru(NCCH_3)_3][PF_6]$ in the presence of light, a different reaction outcome is observed. Surprisingly, the main product is not **5**, but a subsequent CO

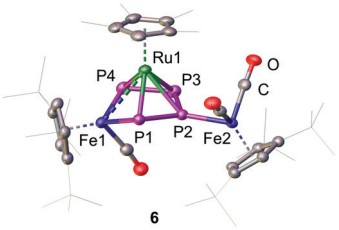

Fig. 2 Cationic part of the 1*S*-2*R*-3*R*-4*R*-5*S* enantiomer of **6** in the solid state. Hydrogen atoms are omitted for clarity. A.d.p. are shown at 50% probability level.

elimination, followed by the insertion of the [Cp‴Fe(CO)] fragment into one of the adjacent P–P bonds, leads to [{Cp‴Fe(CO)$_2$}{Cp‴Fe(CO)}(μ_3,$\eta^{4:2:1}$-P$_4$)(Cp*Ru)][PF$_6$] (**6**) in moderate yield (22%, 70% according to ^{31}P NMR spectroscopy). Complex **6** features a metallo-tetraphosphaene unit and represents a formally twofold activated P$_4$ butterfly complex **1**. The formation of **6** also highlights the high diversity in different binding modes of the P$_4$ unit in **1**. Furthermore, **6** should be handled with caution, as further treatment with UV light leads to subsequent transformations and finally to decomposition.

The insertion of Fe1 into the P1–P4 bond leads to the formation of the 1*S*-2*R*-3*R*-4*R*-5*S* configuration (Fig. 2) while insertion into the P3–P4 bond leads to the formation of the 1*R*-2*S*-3*S*-4*S*-5*R* configuration (Fig. S5, ESI†). The two enantiomers form a racemate and are both present in the solid state structure. The central FeP$_4$ metallacycle reveals an envelope conformation with an almost planar *catena*-P$_4$ unit (dihedral angle P1-P2-P3-P4 of 7.73(3)°). The three Fe–P distances vary from 2.2413(6) to 2.2539(6) Å and are in the range of typical Fe–P single bonds.[21–23] The P–P bond distances vary from 2.1335(8) to 2.1446(8) Å and are in a range between a P–P single and a P=P double bond. The [Cp*Ru] fragment is located over the center of the metallocycle with two shorter Ru–P distances (Ru1–P1 : 2.3592(5); Ru1–P4 : 2.3513(6) Å) and two longer Ru–P distances (Ru1–P2 : 2.4454(5); Ru1–P3 2.4469(6) Å). This results in a shift of the ruthenium fragment towards the [Cp‴Fe1(CO)] fragment and raises the question of a Ru–Fe interaction. While the Ru1–Fe1 distance of 2.9052(4) Å is longer than a predicted single bond (2.41 Å),[23] the distance is still significantly smaller than the sum of the van der Waals radii (4.90 Å).[26] A complex similar to **6** is for example the dirhodium complex [(Cp$^+$Rh(CO))(μ,$\eta^{4:2}$-P$_4$){Cp$^+$Rh}] (**III**, Cp$^+$ = η^5-C$_5$Me$_4$Et).[11] Although, **III** has two electrons more than **6**, the P–P bond lengths (2.150(3)–2.160(3) Å) are comparable. However, in **III**, no metal–metal interaction was observed since the η^4-coordinated [Cp$^+$Rh] fragment is located over the center of the P$_4$ chain. The complex [K(dme)$_2$][(^{Mes}BIAN)Co(μ,$\eta^{4:2}$-P$_4$)Ga(nacnac)][27] (**IV**, dme = dimethoxyethane, ^{Mes}BIAN = 1,2-bis(2,4,6-dimethylphenylimino)acenaphthene, nacnac = CH[CMeN(2,6-^{i}Pr$_2$C$_6$H$_3$)]$_2$) exhibits a similar, however main group-based, heteroatomic core, but without significant metal–metal interaction. The bond lengths (2.1198(7)–2.1286(7) Å) are comparable to the ones in **6**. A similar carbon-based complex is [{CpFe(CO)}{μ,$\eta^{4:2}$-(CR-(CH)$_2$-CR)}(Cp*Ru)] (R = CMe$_2$OH) where the [Cp*Ru] fragment is η^5-coordinated by the cyclopentadiene ring of iron.[28] The reported Ru–Fe distances of 2.6688(7)/2.6743(7) Å are shorter compared to the one in **6** and are described as Ru–Fe single bonds.

The ^{1}H NMR as well as the ^{31}P{^{1}H} NMR spectrum (CD$_2$Cl$_2$) of a crystalline sample of **6** points to the presence of two conformers in solution which are formed in a ratio of 1 : 1.7. At room temperature, both conformers are involved in dynamic processes leading to signal broadening. This is most likely caused by the rotation of either one of the Cp‴ ligands or the whole [Cp‴Fe(CO)$_2$] fragment. At lower temperatures, the rotation is slowed down resulting in sharp signals.‡ The ^{31}P{^{1}H} NMR spectrum shows an AMXY spin system for both isomers which resonate at similar chemical shifts so that they mainly overlap. The signals at δ = 501.1, 465.5, 144.1 and 126.0 ppm can be assigned to the main species while the signals at δ = 500.9, 457.0, 145.2 and 126.5 ppm correspond to the minor species. With chemical shifts and coupling constants (Table S7, ESI†) being almost identical, the structure of the two species must be very similar.‡ However, these findings compare well to [(Cp″Fe)(μ,$\eta^{5:2}$-P$_4$){Cp″Fe(CO)}][8] (δ = 567.2 and 169.1 ppm) and **IV**[27] (δ = 74.0 and −125.4 ppm) showing both an AA′XX′ spin system for the *catena*-P$_4$ unit. The dirhodium complex **III**[11] (δ = 201.4 and 150.8 ppm) reveals an AA′NMXX′ spin system (N and M correspond to Rh).

To obtain deeper insight into the electronic structure of **6**, DFT calculations at the BP86/def2-TZVP level were performed which show the absence of a direct Ru1–Fe1 bond. Instead, a multi-center bond with bond contributions of Ru1 = 40%, Fe1 = 25% and P1 = P4 = 17.5% is present. The Wiberg Bond Index of the Ru1–Fe1 bond of only 0.32 is in good agreement with the multi-center bond description. The corresponding localised molecular orbital, which contains 41% Ru, 24% Fe and 35% P atomic orbital contribution, is depicted in Fig. 3 (left). We could not locate a bond-critical point between Ru and

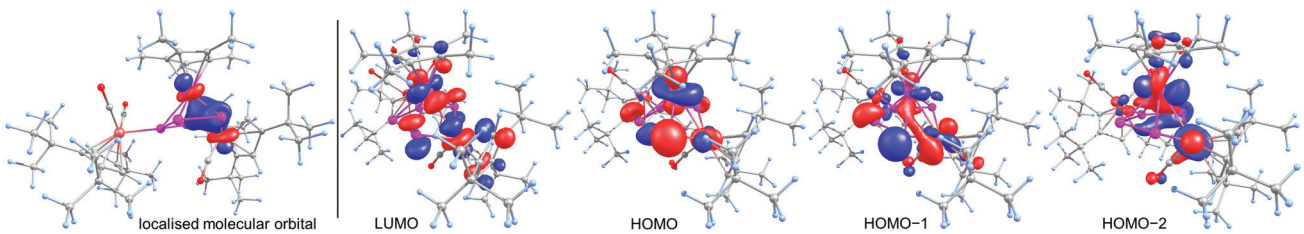

Fig. 3 Left: The localised molecular orbital of **6** showing the interaction between Ru, Fe and P. Right: Frontier orbitals in **6** at the BP86/def2-TZVP level.

Fe1 by the analysis of the topology of the electron density of **6** by means of the Atoms in Molecules (AIM) approach. However, a ring-critical point could be detected, situated in the plane spanned by Ru, Fe1, P1 and P4. The frontier orbitals in **6** are depicted on the right hand side in Fig. 3. The highest occupied molecular orbital (HOMO) shows mainly the lone pairs of the phosphorus atoms while both HOMO−1 and HOMO−2 show mainly bonding interaction within the P_4Fe unit. The lowest unoccupied molecular orbital (LUMO) shows mainly nonbonding orbitals at the phosphorus as well as the metal atoms.

Furthermore, we were interested in why **5** transforms into **6**, while the transformation from **2** to the hypothetical complex $[\{Cp'''Fe(CO)_2\}\{Cp'''Fe(CO)\}(\mu_3,\eta^{4:2:1}\text{-}P_4)(CymRu)]^{2+}$ (**7**) is not observed under the same conditions. Therefore, we determined the natural charge distribution of the four complexes.‡ According to this, the $[CymRu]^{2+}$ fragments act as weak electron acceptors, while $[Cp^*Ru]^+$ act as strong electron acceptors. In contrast, the *cyclo*-P_4R_2 (R = $Cp'''Fe(CO)_2$) units in **2** and **5** act as strong electron donors. During the transformation from *cyclo*-P_4R_2 units to *catena*-P_4 units, this effect is even enhanced. Therefore, it is suggested that the further transformation is dependent on the nature of the ligands that are attached to the central Lewis acid.

The disfavored formation of **7** in comparison to **6** is also highlighted by the calculated reaction energies at the B3LYP level (solvation effects incorporated by the COSMO model). The calculations showed that the formation of **6** starting from **5** is endothermic by 95.87 kJ mol^{-1}. However, these calculations do not take into account the terms of entropy which should have a mayor impact due to the release of CO gas during this process. The formation of **7** starting from **2** would be endothermic by 150.87 kJ mol^{-1} which shows that, in principle, the formation of **6** in comparison to **7** would be energetically less disfavored.

In summary, we could show that the P_4 butterfly complex **1** can easily be activated by a vast variety of different d^6 metal-based Lewis acids, leading to the formation of **2–5** bearing *cyclo*-P_4R_2 units. However, by using $[Cp^*Ru(NCCH_3)_3][PF_6]$ in the presence of light **6** is formed. Complex **6** exhibits an iron-tetraphosphaene unit which is formed *via* CO elimination and the subsequent insertion of the iron fragment into a P–P bond. However, this second activation step is not observed for complexes **2–4** under the same reaction conditions. DFT calculations confirmed that the transformation is strongly dependent on the nature of the ligand at the Lewis acid. The formation of different complexes under mild conditions highlights the high diversity of binding modes of the P_4 unit in **1**.

This work was supported by the Deutsche Forschungsgemeinschaft (Sche 384/38-1).

Conflicts of interest

There are no conflicts to declare.

Notes and references

‡ See ESI† for further information.

1 C. Chow, M. Taoufik and E. A. Quadrelli, *Eur. J. Inorg. Chem.*, 2011, 1349.
2 (*a*) D. W. Stephan, *Dalton Trans.*, 2009, 3129; (*b*) G. C. Welch, R. R. S. Juan, J. D. Masuda and D. W. Stephan, *Science*, 2006, **314**, 1124.
3 (*a*) D. M. Ermert and L. J. Murray, *Dalton Trans.*, 2016, **45**, 14499; (*b*) N. Hazari, *Chem. Soc. Rev.*, 2010, **39**, 4044.
4 (*a*) M. Behrens, *Angew. Chem., Int. Ed.*, 2014, **53**, 12022; (*b*) V. P. Indrakanti, J. D. Kubicki and H. H. Schobert, *Energy Environ. Sci.*, 2009, **2**, 745.
5 (*a*) M. Scheer, G. Balázs and A. Seitz, *Chem. Rev.*, 2010, **110**, 4236; (*b*) N. A. Giffin and J. D. Masuda, *Coord. Chem. Rev.*, 2011, **255**, 1342.
6 (*a*) B. M. Cossairt, N. A. Piro and C. C. Cummins, *Chem. Rev.*, 2010, **110**, 4164; (*b*) M. Caporali, L. Gonsalvi, A. Rossin and M. Peruzzini, *Chem. Rev.*, 2010, **110**, 4178.
7 (*a*) S. Heinl, A. Y. Timoshkin, J. Müller and M. Scheer, *Chem. Commun.*, 2018, **54**, 2244; (*b*) M. Scheer, K. Schuster and U. Becker, *Phosphorus, Sulfur Silicon Relat. Elem.*, 1996, **109**, 141.
8 O. J. Scherer, G. Schwarz and G. Wolmershäuser, *Z. Anorg. Allg. Chem.*, 1996, **622**, 951.
9 O. J. Scherer, T. Hilt and G. Wolmershäuser, *Organometallics*, 1998, **17**, 4110.
10 S. Dürr, D. Ertler and U. Radius, *Inorg. Chem.*, 2012, **51**, 3904.
11 O. J. Scherer, M. Swarowsky, H. Swarowsky and G. Wolmershäuser, *Angew. Chem., Int. Ed. Engl.*, 1988, **27**, 694.
12 J. J. Weigand, M. Holthausen and R. Fröhlich, *Angew. Chem., Int. Ed.*, 2009, **48**, 295.
13 O. J. Scherer, M. Swarowsky and G. Wolmershaeuser, *Organometallics*, 1989, **8**, 841.
14 B. Zarzycki, F. M. Bickelhaupt and U. Radius, *Dalton Trans.*, 2013, **42**, 7468.
15 O. J. Scherer, T. Dave, J. Braun and G. Wolmershäuser, *J. Organomet. Chem.*, 1988, **350**, C20–C24.
16 M. Modl, S. Heinl, G. Balázs, F. Delgado Calvo, M. Caporali, G. Manca, M. Keilwerth, K. Meyer, M. Peruzzini and M. Scheer, *Chem. – Eur. J.*, 2019, **25**, 6300.
17 (*a*) D. Yakhvarov, P. Barbaro, L. Gonsalvi, S. Mañas Carpio, S. Midollini, A. Orlandini, M. Peruzzini, O. Sinyashin and F. Zanobini, *Angew. Chem., Int. Ed.*, 2006, **45**, 4182; (*b*) M. Di Vaira, M. P. Ehses, M. Peruzzini and P. Stoppioni, *Eur. J. Inorg. Chem.*, 2000, 2193; (*c*) A. P. Ginsberg and W. E. Lindsell, *J. Am. Chem. Soc.*, 1971, **93**, 2082.
18 J. J. Schneider, D. Wolf, C. Janiak, O. Heinemann, J. Rust and C. Krüger, *Chem. – Eur. J.*, 1998, **4**, 1982.
19 C. Schwarzmaier, A. Y. Timoshkin, G. Balázs and M. Scheer, *Angew. Chem., Int. Ed.*, 2014, **53**, 9077.
20 (*a*) O. J. Scherer, T. Hilt and G. Wolmershäuser, *Angew. Chem., Int. Ed.*, 2000, **39**, 1425; (*b*) M. Scheer, S. Deng, O. J. Scherer and M. Sierka, *Angew. Chem., Int. Ed.*, 2005, **44**, 3755.
21 C. Schwarzmaier, S. Heinl, G. Balázs and M. Scheer, *Angew. Chem., Int. Ed.*, 2015, **54**, 13116.
22 (*a*) J. Müller, S. Heinl, C. Schwarzmaier, G. Balázs, M. Keilwerth, K. Meyer and M. Scheer, *Angew. Chem., Int. Ed.*, 2017, **56**, 7312; (*b*) J. Müller and M. Scheer, *Chem. – Eur. J.*, 2021, 26, DOI: 10.1002/chem.202005025.
23 P. Pyykkö and M. Atsumi, *Chem. – Eur. J.*, 2009, **15**, 186.
24 F. Kraus, J. C. Aschenbrenner and N. Korber, *Angew. Chem., Int. Ed.*, 2003, **42**, 4030.
25 (*a*) C. Anthony, S.-M. Nathalie, N. Noel, F.-B. Marie and M. Nicolas, *Angew. Chem., Int. Ed.*, 2018, **57**, 1874; (*b*) U. Chakraborty, J. Leitl, B. Muhldorf, M. Bodensteiner, S. Pelties and R. Wolf, *Dalton Trans.*, 2018, **47**, 3693; (*c*) F. Dielmann, A. Timoshkin, M. Piesch, G. Balázs and M. Scheer, *Angew. Chem., Int. Ed.*, 2017, **56**, 1671; (*d*) M. Piesch, S. Reichl, M. Seidl, G. Balázs and M. Scheer, *Angew. Chem., Int. Ed.*, 2019, **58**, 16563; (*e*) O. J. Scherer, R. Winter and G. Wolmershäuser, *Z. Anorg. Allg. Chem.*, 1993, **619**, 827.
26 S. Alvarez, *Dalton Trans.*, 2013, **42**, 8617.
27 C. G. P. Ziegler, T. M. Maier, S. Pelties, C. Taube, F. Hennersdorf, A. W. Ehlers, J. J. Weigand and R. Wolf, *Chem. Sci.*, 2019, **10**, 1302.
28 J. N. L. Dennett, S. A. R. Knox, K. M. Anderson, J. P. H. Charmant and A. G. Orpen, *Dalton Trans.*, 2005, 63.

